(RESEARCH ARTICLE)

Check for updates

Molecular Geometry, Bond Length, Bond Angle, FT-IR, UV Visible, HOMO-LUMO of 1,3-diphenyl-3-(phenylamino) propan-1-one by Using Density Functional Theory

RAGAVI.R *, RAJESH.P, VIGNESH.N and BASKARAN.M

Research scholar, PG and Research, Department of Chemistry, Government Arts College (Autonomous), Coimbatore – 641018, Tamilnadu, India.

Abstract

The quantum chemical calculations of organic compound 1,3-diphenyl-3-(phenylamino) propan-1-one has been performed by density functional theory (DFT) using the B3LYP method with 6-311G (d,p) basis set. The electronic properties such as Frontier orbital and band gap energies have been calculated using DFT. The global reactivity descriptor has been computed to predict chemical stability and reactivity of the molecule. The computational studies, via optimization of molecular geometry, stimulated vibrational frequency, UV-Vis absorbance, different partial atomic charges, surface analyses, bond Length (Å), bond angle, FT-IR, UV Visible, HOMO-LUMO, FMO analyses, were also carried out using B3LYP/6-31G(d,p) basic set. The computational attempts of the target molecule were made with deep insights toward their future scope comprising chemical reactivity, biological property, and optical device applications.

Keywords: Density Functional Theory; Bond Length; Bond Angle; FT-IR; UV-Visible; Gaussian 16; HOMO-LUMO

1. Introduction

Mannich-type of reaction is one of the greatest vital carbon-carbon bond-making reactions for the preparation of the secondary and tertiary amine derivatives. The β-amino carbonyl compounds are the outcomes of Mannich reaction, which have been employed for the preparation of peptides, lactams, and precursors to optically active amino acids. The products of Mannich reactions are most suitable intermediates in medicinal applications and natural materials synthesis; these intermediates are used in drug synthesis, viz., antimalarial, antitumor, antihypertensive etc. agents.[1,2,3,4,5] Many schemes that have been examined as catalysts for the Mannich reaction over the several earlier decades, viz., Lewis acids,[6,7,8,9,10], Bases, [11,12,13,14] Brønsted acids,[2,15,16,17,18] which often suffer from the disadvantages of elongated reaction times, harsh reaction circumstances, poisonousness and complication in the product purification. Hence, the search for innovative and user-friendly catalysts is energetically tracked. Recently, triazolium based ionic liquids [19] were used as catalysts for the synthesis of β-amino carbonyl compounds with high yield. In general, β-amino carbonyl compounds have a secondary amine functional group which is potentially utilized for the sensing of anions. The target molecule 1,3-diphenyl-3-(phenylamino) propan-1-one poses both NH and C=O functional groups to enhance its sensing ability. Every molecule possesses some hidden properties based upon their electronic interactions with neighboring atoms and their biological activities are based on these interactions. An important emerging technique is computational quantum mechanical modeling [20]. The DFT approach is broadly used in order to explain the multi electron systems on a quantum level. The stable molecular geometry of 1,3-diphenyl-3-(phenylamino)propan-1-one in the state of minimum energy was optimized and the bond parameters were calculated by Gaussian 16 and DFT, B3LYP/6–31 + G(d,p)[21,22] and basis sets, Molecular electrostatic potential, FMO (HOMO to LUMO), and some global descriptors were theoretically analyzed by using DFT level of theory to obtain the electronic properties of the titled compound [23,24]. DFT calculations are the most important method to determine the behaviour

* Corresponding author: RAJESH.P.

of a molecule, Since there is lot of research have been reported on the usage of the gas phase but nominal work have done with different solvents phase, So we focused to investigate the influence of solvent polarity on the structural and electronic properties of 1,3-diphenyl-3-(phenylamino)propan-1-one, DFT studies were carried out in the gas phase as well as in DMSO and DCM medium using the B3LYP functional with the 6-311++G(d,p) basis set. From these calculations, several bond parameters like bond angle, bond length can be calculated and also able to explore the activities of the selected molecule. In the present study, 1,3-diphenyl-3-(phenylamino) propan-1-one was synthesized and characterized utilizing various analytical techniques such as Bond Length (Å), Bond Angle, FT-IR, UV Visible, HOMO-LUMO were carried out for identifying the purity of the target molecule. The DFT studies including stimulated vibrational frequency and UV-Vis spectral analyses were carried out using B3LYP /6-31G (d,p) basis set.

2. Material and methods

2.1. Experimental

The quantum chemical calculations of 1,3-diphenyl-3-(phenylamino) propan-1-one was executed by applying DFT method B3LYP with 6-311G (d,p) basis set using Gaussian 16 software.

2.2. Computational studies

 The quantum chemical calculation has been performed in the Gaussian 16 program package with the help of DFT [25,26]. The structure of the molecule was optimized by the DFT using hybrid functional B3LYP (Becke's three-parameter exchange functional [27] combined with Lee-Yang-Parr correlation functional [28] with the 6-31G (d,p) basis set [29]. The optimized parameters are performed as vibrational frequency calculation in the DFT to characterize all the stationary points as minima [30]. The B3LYP method is used to evaluate the molecular electrostatic potential of reactive sites of title compounds. The HOMO-LUMO energies are predicted by using the DFT approach [23].The molecular geometry is optimized without any restriction.

3. Results and discussion

3.1. Theoretical analysis

DFT calculations are used to optimize the 1,3-diphenyl-3-(phenylamino) propan-1-one structure. The B3LYP hybrid functional along with a 6-31+G* basis set for carbon (C), nitrogen (N), oxygen (O), and hydrogen (H) were employed. The optimized geometry is characterized by only real frequencies as given in Figure1 and the corresponding atom numbers, as labelled in Figure 2. Table-1 and 2 show the bond length and angle parameters for1,3-diphenyl-3-(phenylamino) propan-1-one. The DFT calculations are carried out using the Gaussian16 software.
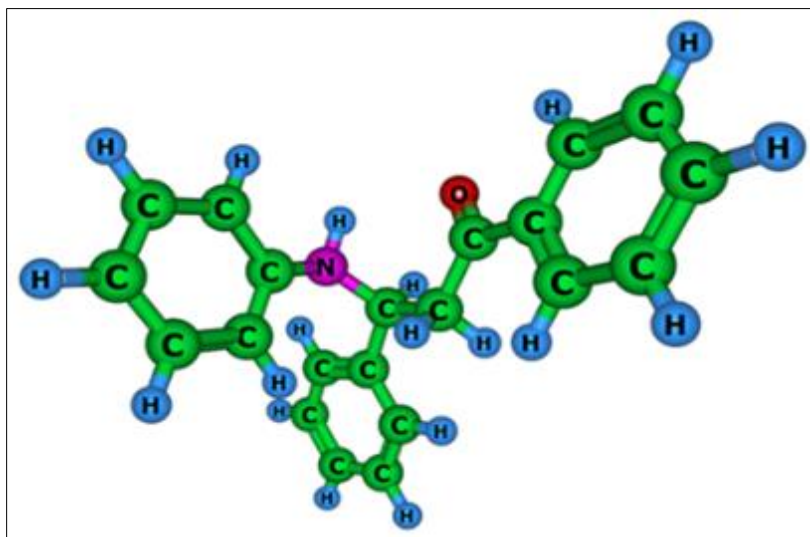

Figure 1 Optimized geometry of 1,3-diphenyl-3-(phenylamino) propan-1-one
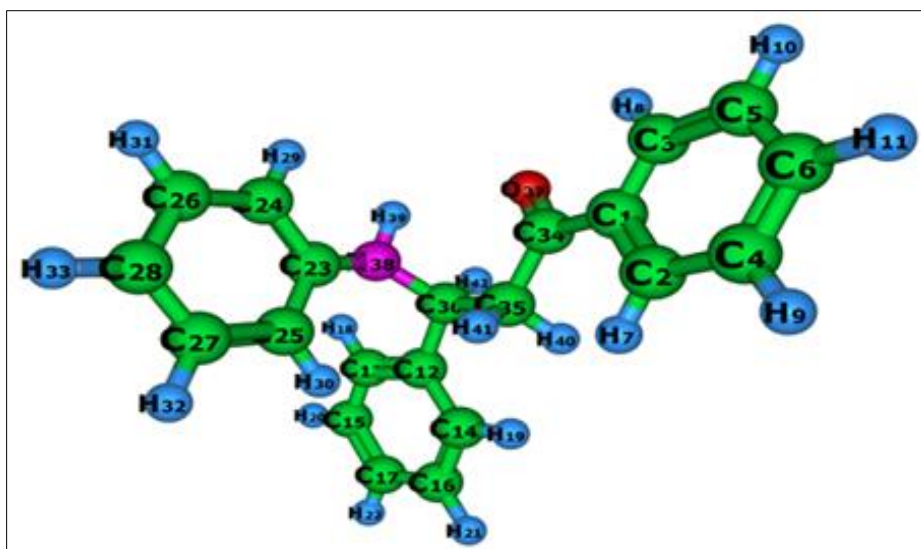
Figure 2 Optimized geometry of 1,3-diphenyl-3-(phenylamino) propan-1-one with labelling of atom numbers

3.2. Bond lengths

Bond lengths are critical indicators of the electron delocalization and hybridization state of atoms in a molecule. The observed values (Table 1) indicate standard C–C, C–H, C=O, and C–N bond characteristics.

Table 1 The bond length (Å) for 1,3-diphenyl-3-(phenylamino) propan-1-one with gas and two different solvent phases

Structure	Atoms	Bond Length (Å)		
		Gas phase	Dimethylsulfoxide	Dichloromethane
1,3-diphenyl-3-(phenylamino) propan-1-one	C_1-C_2	1.405	1.406	1.406
	C_1-C_3	1.406	1.407	1.407
	C_3-C_5	1.393	1.393	1.393
	C_5-C_6	1.400	1.401	1.401
	C_2-C_4	1.396	1.397	1.397
	C_4-C_6	1.397	1.398	1.398
	C_3-H_8	1.080	1.080	1.080
	C_5-H_{10}	1.080	1.080	1.080
	C_6-H_{11}	1.080	1.080	1.080
	C_4-H_9	1.080	1.080	1.080
	C_2-H_7	1.080	1.080	1.080
	C_1-C_{34}	1.499	1.540	1.540
	C_{34}-O_{37}	1.220	1.220	1.220
	C_{34}-C_{35}	1.540	1.540	1.540
	C_{35}-H_{40}	1.080	1.080	1.080
	C_{35}-H_{41}	1.080	1.080	1.080
	C_{35}-C_{36}	1.542	1.540	1.540
	C_{36}-H_{42}	1.097	1.080	1.080

	$C_{36}-C_{12}$	1.535	1.540	1.540
	$C_{36}-N_{38}$	1.470	1.470	1.470
	$N_{38}-H_{39}$	1.000	1.000	1.000
	$C_{12}-C_{13}$	1.405	1.405	1.405
	$C_{12}-C_{14}$	1.402	1.402	1.402
	$C_{14}-C_{16}$	1.400	1.401	1.401
	$C_{16}-C_{17}$	1.395	1.396	1.396
	$C_{17}-C_{15}$	1.399	1.400	1.400
	$C_{15}-C_{13}$	1.395	1.396	1.395
	$C_{13}-H_{18}$	1.086	1.080	1.080
	$C_{15}-H_{20}$	1.087	1.080	1.080
	$C_{17}-H_{22}$	1.087	1.080	1.080
	$C_{16}-H_{21}$	1.087	1.080	1.080
	$C_{14}-H_{19}$	1.086	1.080	1.080
	$N_{38}-C_{23}$	1.402	1.470	1.470
	$C_{23}-C_{24}$	1.411	1.414	1.413
	$C_{24}-C_{26}$	1.393	1.393	1.393
	$C_{26}-C_{28}$	1.400	1.401	1.401
	$C_{28}-C_{27}$	1.396	1.398	1.397
	$C_{27}-C_{25}$	1.398	1.399	1.399
	$C_{23}-C_{25}$	1.409	1.410	1.410
	$C_{24}-H_{29}$	1.080	1.080	1.080
	$C_{26}-H_{31}$	1.080	1.080	1.080
	$C_{28}-H_{33}$	1.080	1.080	1.080
	$C_{27}-H_{32}$	1.080	1.080	1.080
	$C_{25}-H_{30}$	1.080	1.080	1.080

Table 2 The bond angle for 1,3-diphenyl-3-(phenylamino) propan-1-one with gas and solvent phases

Structure	Atoms	Bond Angle		
		Gas phase	DMSO solvent	DCM solvent
1,3-diphenyl-3-(phenylamino) propan-1-one	C_1-C_3-H_8	118.48	118.88	118.82
	H_8-C_3-C_5	120.99	120.54	120.60
	C_3-C_5-H_{10}	119.90	119.92	119.91
	H_{10}-C_5-C_6	120.06	120.10	120.09
	H_{11}-C_6-C_4	120.00	120.01	120.01
	C_6-C_4-H_9	120.16	120.17	120.17
	H_9-C_4-C_2	119.78	119.72	119.74
	C_4-C_2-H_7	119.01	118.92	118.93
	H_7-C_2-C_1	120.55	120.69	120.66
	C_1-C_{34}-O_{37}	120.28	120.39	120.39
	O_{37}-C_{34}-C_{35}	120.85	120.84	120.82
	H_{41}-C_{35}-H_{40}	106.34	106.14	106.19
	C_{35}-C_{36}-H_{42}	106.19	106.30	106.26
	H_{42}-C_{36}-C_{12}	106.08	103.38	105.94
	C_{36}-N_{38}-H_{39}	109.95	110.53	110.41
	C_{36}-C_{12}-C_{13}	118.44	118.20	118.22
	H_{18}-C_{13}-C_{15}	120.13	119.81	119.87
	H_{20}-C_{15}-C_{17}	120.09	120.11	120.11
	C_{15}-C_{17}-H_{22}	120.41	120.36	120.37
	C_{17}-C_{16}-H_{21}	120.19	120.19	120.19
	H_{21}-C_{16}-C_{14}	119.47	119.44	119.45
	C_{16}-C_{14}-H_{19}	118.27	118.41	118.39
	H_{19}-C_{14}-C_{12}	120.74	120.69	120.70
	N_{38}-C_{23}-C_{24}	118.48	118.41	118.42
	C_{23}-C_{24}-H_{29}	119.13	119.14	119.13
	H_{29}-C_{24}-C_{26}	119.80	119.77	119.77
	H_{31}-C_{26}-C_{28}	120.14	120.13	120.14
	C_{26}-C_{28}-H_{33}	120.66	120.69	120.69
	C_{28}-C_{27}-H_{32}	119.97	119.99	119.98
	C_{27}-C_{25}-H_{30}	119.30	119.18	119.22

The molecule's atomic charge distribution is described by Mulliken population analysis. Figure-3: displays the atomic charge distribution of the 1,3-diphenyl-3-(phenylamino) propan-1-one. The neighboring N and H atoms exhibit a positive neutralization zone, whereas the C atoms exhibit a negative zone.
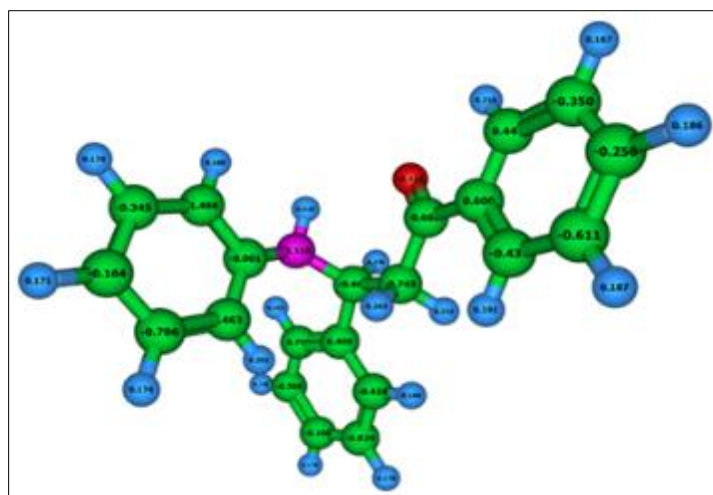
Figure 3 Mulliken charge of 1,3-diphenyl-3-(phenylamino) propan-1-one

3.3. Frontier Molecular Orbital (FMO) Analysis of 1,3-diphenyl-3-(phenylamino) propan-1-one

3.3.1. Frontier Molecular Orbital Visualization

The energy levels of the highest-occupied (HOMO) and lowest-unoccupied (LUMO) molecular orbitals are extremely valuable in determining the structure's stability and reactivity. The HOMO-LUMO energy gaps (H-L gap) are calculated using the LUMO-HOMO energy difference. However, a larger H-L gap indicates that the structure is more stable. Figure 4 displays the HOMO-LUMO plots (contour value is 0.03 a.u.) and Table-3 provides the H-L gap values of the gas and solvent phases structures.
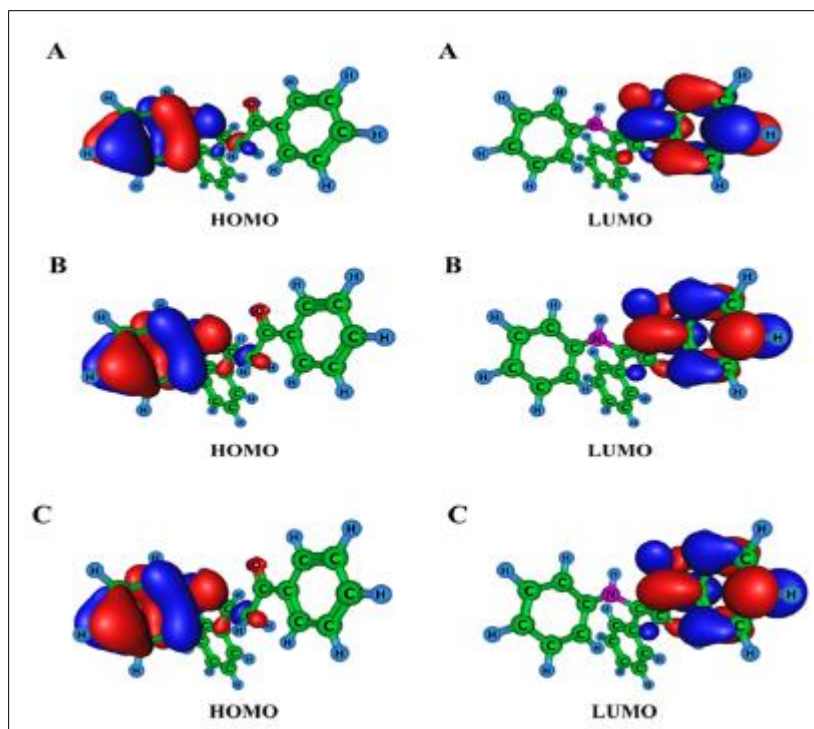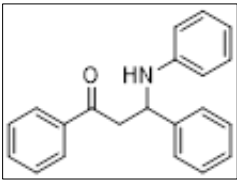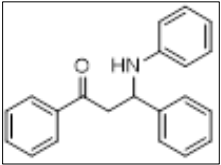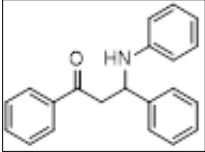

Figure 4 A) HOMO-LUMO plots of 1,3-diphenyl-3-(phenylamino) propan-1-one, B) HOMO-LUMO plots of 1,3-diphenyl-3-(phenylamino) propan-1-one with Dimethyl sulfoxide, C) HOMO-LUMO plots of 1,3-diphenyl-3-(phenylamino) propan-1-one with Dichloromethane

Figure 4 Shows the molecular orbital's phase, with red signifying the positive phase and blue the negative phase. The HOMO is primarily localized over the electron-rich aromatic ring and amine group region. This indicates a high electron-donating ability from these areas. The LUMO is predominantly spread across the carbonyl group (C=O) and adjacent phenyl ring, which are electron-deficient. This signifies a strong electrophilic character, implying that this region could serve as an acceptor during intramolecular or intermolecular electron transfer. Thus, the 1,3-diphenyl-3-(phenylamino) propan-1-one with the Dimethyl Sulfoxide structure (3.62 eV) has a higher H-L gap, which implies that it is more stable than the 1,3-diphenyl-3-(phenylamino) propan-1-one with Dichloromethane (3.53eV) and the 1,3-diphenyl-3-(phenylamino) propan-1-one (2.42 eV)

Table 3 Total energy and HOMO-LUMO gap values of 1,3-diphenyl-3-(phenylamino) propan-1-one with gas and solvent phases

Structure	Total energy (in Hartree)	HOMO (eV)	LUMO (eV)	HOMO-LUMO gap (eV)
 1,3-diphenyl-3-(phenylamino) propan-1-one with gas phase	-941.686552	-4.64	-2.22	2.42
 1,3-diphenyl-3-(phenylamino) propan-1-one with Dimethyl sulfoxide	-941.6979782	-5.68	-2.05	3.62
 1,3-diphenyl-3-(phenylamino)propan-1-one with Dichloromethane	-941.6960461	-5.60	-2.07	3.53

3.4. UV-Visible Spectral Analysis of 1,3-diphenyl-3-(phenylamino) propan-1-one

The UV-Visible absorption spectrum of the synthesized 1,3-diphenyl-3-(phenylamino) propan-1-one was recorded in the range of 200–500 nm. The compound exhibited a strong absorption maximum at 267.06 nm with an intensity of approximately 2100 arbitrary units (a.u.). A secondary, much weaker and broader absorption band was also observed in the region between 400–450 nm. The spectrum is presented in Figure 5.
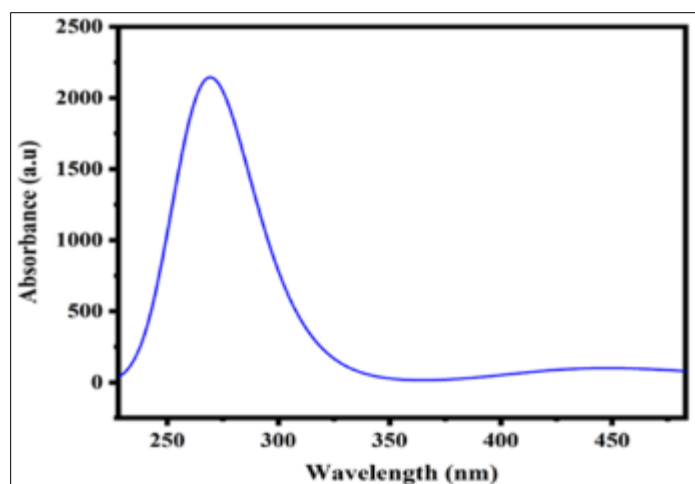
Figure 5 Absorption plot of 1,3-diphenyl-3-(phenylamino) propan-1-one (maximum absorption wavelength = 267.06 nm)
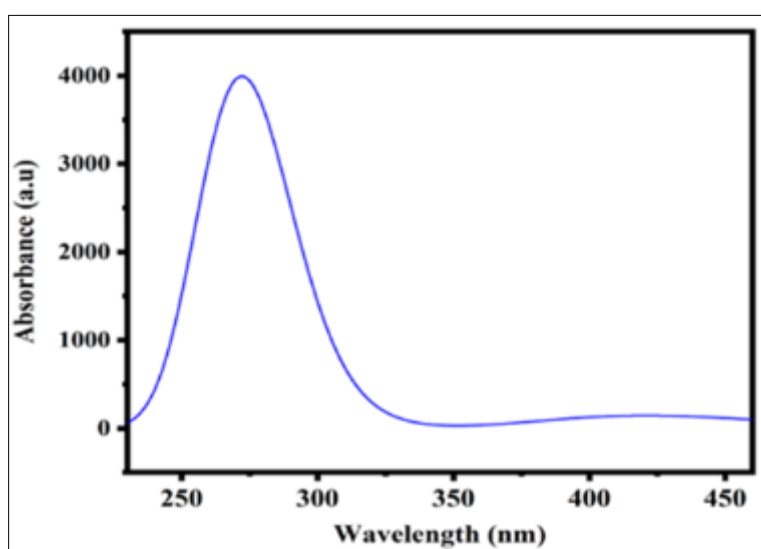

Figure 6 Absorption plot of 1,3-diphenyl-3-(phenylamino) propan-1-one-DMSO (maximum absorption wavelength = 269.49 nm)

3.5. Electronic Transitions and Interpretation

3.5.1. Major Band at 267.06 nm – π→π* Transitions

The intense absorption peaks at 267.06 nm and 269.49 nm are primarily attributed to π→π* electronic transitions, typical of aromatic compounds and molecules possessing conjugated π-systems. The 1,3-diphenyl-3-(phenylamino) propan-1-one structure contains multiple phenyl rings conjugated to a central carbonyl functionality, facilitating such transitions. The π→π* transitions are known to be intense due to allowed transitions between bonding and antibonding π-molecular orbitals. These phenyl groups provide an extended conjugation path, which lowers the HOMO-LUMO energy gap and allows strong π→π* absorption in the near-UV region. The minor redshift in DMSO can be attributed to solvent effects DMSO stabilizes the excited state more than the ground state due to its polar nature, resulting in a smaller energy gap and thus a shift to a longer wavelength. Upon dissolving the compound in DMSO, a polar aprotic solvent, a distinct bathochromic shift was observed, with the maximum absorption wavelength shifting to 269.49 nm. The intensity of absorption also increased significantly, with a peak value close to 4000 a.u. (Figure 6). This solvent-dependent spectral variation highlights the solvatochromic behavior of the 1,3-diphenyl-3-(phenylamino)propan-1-one.

3.5.2. Influence of Molecular Structure on Absorption

The absorption profile is significantly influenced by the conjugation between the carbonyl and aromatic groups, the electron-donating nature of the phenylamino (-NH-Ph) group at the β-position, and possible intramolecular charge transfer (ICT) interactions. These factors stabilize the π-system and shift the absorption to longer wavelengths.

3.5.3. Minor Band between 400–450 nm – n→π* Transitions

A broad and weak band in the 400–450 nm region may arise due to n→π* transitions. These transitions occur when non-bonding (n) electrons from heteroatoms such as carbonyl oxygen or amino nitrogen are excited to π* antibonding orbitals. These transitions are known to be of lower intensity and more sensitive to solvent.

3.5.4. Solvent Effects on Absorption Behaviour

The comparative spectra reveal that the 1,3-diphenyl-3-(phenylamino) propan-1-one displays modest solvatochromism. In polar solvents like DMSO, the π→π* transition band shifts to a slightly longer wavelength (269.49 nm from 267.06 nm) and increases in intensity. This bathochromic shift arises from differential stabilization of the ground and excited states by the solvent. Polar solvents stabilize the polar excited states more than the ground states, lowering the transition energy.

3.5.5. Vibrational Spectral Analysis of 1,3-diphenyl-3-(phenylamino) propan-1-one

The vibrational (IR) spectrum of the 1,3-diphenyl-3-(phenylamino) propan-1-one, calculated using DFT methods, displays distinct absorption bands across the range of 400–4000 cm^{-1}. The spectrum (Figure 7) is characterized by high-intensity peaks in the fingerprint region (600–1800 cm^{-1}) as well as moderate absorptions in the higher frequency region (3000–3600 cm^{-1}), corresponding to various functional groups within the molecule. Observed the C=O stretching sharp and intense peak near 1700–1750 cm^{-1} corresponds to the carbonyl stretching vibration. This mode is characteristic of ketonic C=O bonds and is strongly IR-active due to a significant change in dipole moment. And the N-H stretching medium intensity peaks comes around 3300–3400 cm^{-1} are attributed to the N-H stretching vibrations of the secondary amine group. These bands may be slightly broadened due to hydrogen bonding. The C-H aromatic stretching peaks in the range of 3000–3080 cm^{-1} are indicative of aromatic C-H stretches, arising from the phenyl groups in the molecule. The C=C aromatic ring stretching showed intense absorptions in the region of 1500–1600 cm^{-1} are associated with C=C skeletal stretching of the phenyl rings. These peaks are typically sharp and intense, helping confirm aromatic character. Bands near 1200–1400 cm^{-1} correspond to C-N stretching, especially from the phenylamino substituent, along with coupled N-H bending vibrations. Then the Low-frequency peaks below 1000 cm^{-1} arise from out-of-plane aromatic ring deformations and other complex bending modes of the molecular skeleton.
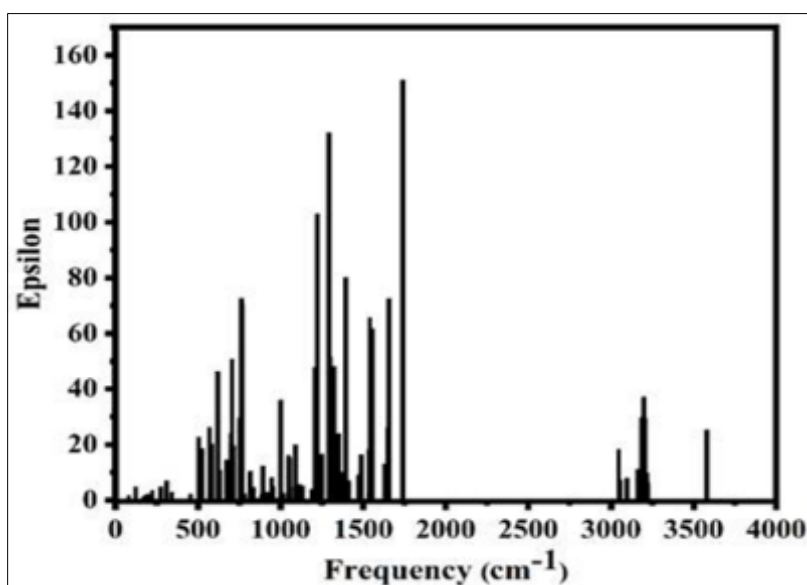

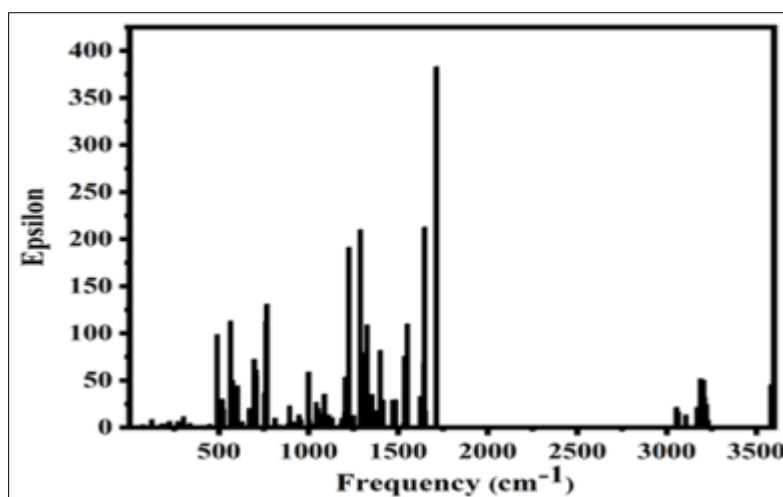**Figure 7** IR plot of 1,3-diphenyl-3-(phenylamino) propan-1-one

Figure 8 IR plot of 1,3-diphenyl-3-(phenylamino) propan-1-one -DMSO

4. Conclusion

DFT calculations at the B3LYP/6-311++G(d,p) level was employed to examine the structural and electronic characteristics of 1,3-diphenyl-3 phenylamino) propan-1-one in three different environments: gas phase, DCM, and DMSO. The results showed minor elongation in bond lengths and small deviations in bond angles upon solvation, which can be attributed to solvent-induced electronic relaxation. FMO analysis revealed that the HOMO–LUMO energy gap decreased slightly in solvents compared to the gas phase. Among the solvents, DMSO showed the lowest energy gap, suggesting improved electron delocalization and enhanced molecular reactivity in a polar environment. Mulliken charge distribution further supported this observation by showing a more significant shift in atomic charges, especially at the carbonyl and amino sites, in DMSO. This indicates stronger solute–solvent interactions and higher charge separation. Based on the combined analysis of geometrical parameters, FMO energies, and Mulliken charges, DMSO emerged as the most stabilizing solvent for the title compound. It is therefore recommended for further theoretical and experimental work involving this molecule.

Compliance with ethical standards

Disclosure of conflict of interest

The Author declares that there is no conflict of interest regarding the publication of this article.

References

[1] S. G. Subramanipillai, "Mannich Reaction: A Versatile and Convenient Approach to Bioactive Skeletons," Journal of Chemical Sciences 125 (2013): 467–82.

[2] A. Najmodin, L. Torkiyan, and R. M. Saidi, "Highly Efficient One-Pot Three-Component Mannich Reaction in Water Catalyzed by Heteropoly Acids," Organic Letters 8, no. 10 (2006): 2079–82.

[3] S. Sahoo, T. Joseph, and S. B. Halligudi, "Mannich Reaction in Bronsted Acidic Ionic Liquid: A Facile Synthesis of b-Amino Carbonyl Compounds," Journal of Molecular Catalysis A: Chemical 244, no. 1–2 (2006): 179–82.

[4] S. Palaniappan, A. John, C. A. Amarnath, and V. J. Rao, "Mannich-Type Reaction in Solvent Free Condition Using Reusable Polyaniline Catalyst," Journal of Molecular Catalysis A: Chemical 218, no. 1 (2004): 47–53.

[5] S. K. Bur, and S. F. Martin, "Mannich Reactions: Selectivity and Synthetic Utility," Tetrahedron 57, no. 16 (2001): 3221–42.

[6] S. Kobayashi, and H. Ishitani, "Catalytic Enantioselective Addition to Imines," Chemical Reviews 99, no. 5 (1999): 1069–94.

[7] R. M€uller, H. Goesmann, and H. Waldmann, "N, N-Phthaloylamino Acids as Chiral Auxiliaries in Asymmetric Mannich-Type Reactions," Angewandte Chemie International Edition 38, no. 1–2 (1999): 184–7.

[8]   A. S. Chiang, C. Y. Lin, C. C. Chuang, H. M. Chang, C. H. Hsieh, C. W. Yeh, C. T. Shih, J. J. Wu, G. T. Wang, Y. C. Chen, et al. "Three-Dimensional Reconstruction of Brain-Wide Wiring Networks in Drosophila at Single-Cell Resolution," Current Biology 8 (2007): 112217–21.

[9]   C. X. Zhang, Z. M. Ge, T. M. Cheng, and R. T. Li, "Synthesis and Analgesic Activity of Secondary Amine Analogues of Pyridylmethylamine and Positional Isomeric Analogues of ABT-594," Bioorganic & Medicinal Chemistry Letters 16, no. 7 (2006): 2013

[10]   T. Ollevier, E. Nadeau, and A. A. Guay-Begin, "Direct-Type Catalytic Three-Component Mannich Reaction in Aqueous Media," Tetrahedron Letters 47, no. 47 (2006): 8351–4.

[11]   W.-J. Hao, B. Jiang, S.-J. Tu, X.-D. Cao, S.-S. Wu, S. Yan, X.-H. Zhang, Z.-G. Han, and F. Shi, "A New Mild Base-Catalyzed Mannich Reaction of Hetero-Arylamines in Water: Highly Efficient Stereoselective Synthesis of Beta-Aminoketones under Microwave Heating," Organic & Biomolecular Chemistry 7, no. 7 (2009): 1410–4.

[12]   P. Goswami, and B. Das, "Adenine as Amino Catalyst for Green Synthesis of Diastereoselective Mannich Products in Aqueous Medium," Tetrahedron Letters 50, no. 20 (2009): 2384–8. S.

[13]   Wei, L.-M. Wang, and H. Tian, "Quaternary Ammonium Salt Gemini Surfactants Containing Perfluoroalkyl Tails Catalyzed One-Pot Mannich Reactions in Aqueous Media," Journal of Fluorine Chemistry 129, no. 4 (2008): 267–73. Y.-S.

[14]   Wu, J. Cai, Z.-Y. Hu, and G.-X. Lin, "A New Class of Metal-Free Catalysts for Direct Diastereo-and Regioselective Mannich Reactions in Aqueous Media," Tetrahedron Letters 45, no. 48 (2004): 8949–52.

[15]   K. Manabe, and S. Kobayashi, "Mannich-Type Reactions of Aldehydes, Amines, and Ketones in a Colloidal Dispersion System Created by a Brønsted Acid-Surfactant-Combined Catalyst in Water," Organic Letters 1, no. 12 (1999): 1965–7.

[16]   D. Fang, "Mannich Reaction in Water Using Acidic Ionic Liquid as Recoverable and Reusable Catalyst," Catalysis Letters 116 (2007): 76–80.

[17]   D. Fang, Z. H. Fei, and Z. L. Liu, "Functionalized Ionic Liquid as Recyclable Catalyst for Mannich Reaction in Aqueous Medium," Catalysis Communications 10 (2009): 1267–70.

[18]   G. Zhao, T. Jiang, H. Gao, B. Han, J. Huang, and D. Sun, "Mannich Reaction Using Acidic Ionic Liquids as Catalysts and Solvents," Green Chemistry 6, no. 2 (2004): 75–7.

[19]   D. Meyer, and T. Strassner, "1,2,4-Triazole-Based Tunable Aryl/Alkyl Ionic Liquids," The Journal of Organic Chemistry 76, no. 1 (2011): 305–8.

[20]   Saeed, S., et al. (2013). "Synthesis, spectroscopic characterization, DFT studies and antimicrobial activity of some new β-ketoenol derivatives." Spectrochimica Acta Part A: Molecular and Biomolecular Spectroscopy, 109, 43–52.

[21]   Tirado-Rives, Julian, and William L. Jorgensen. "Performance of B3LYP density functional methods for a large set of organic molecules." Journal of chemical theory and computation 4, no. 2 (2008): 297-306.

[22]   Computer Program:A Frisch, M. J.A Trucks, G. W.A Schlegel, H. B.A Scuseria, G. E.A Robb, M. A.A Cheeseman, J. R.A Scalmani, G.A Barone, V.A Petersson, G. A.A Nakatsuji, H.A Li, X.A Caricato, A.A Marenich, A. V.A Bloino, J.A Janesko, B. G.A Gomperts, R.A Mennucci, B.A Hratchian, H. P.A Ortiz, J. V.A Izmaylov, A. F.A Sonnenberg, J. L.A WilliamsA Ding, F.A Lipparini, F.A Egidi, F.A Goings, J.A Peng, B.A Petrone,A Henderson, T.A Ranasinghe, D.A Zakrzewski, V. G.A Gao, J.A Rega, N.A Zheng, .A Liang, W.A Hada, M.A Ehara, M.A Toyota, K.A Fukuda, R.A Hasegawa, J.A Ishida, M.A Nakajima, T.A Honda, Y.A Kitao, O.A Nakai, H.%A Vreven, T.A Throssell, K.A Montgomery Jr., J. A,A Peralta, J. E.A Ogliaro, F,A Bearpark, M. J.A Heyd, J. J,A Brothers, E. N,A Kudin, K. N,A Staroverov, V. N,A Keith, T. A,A Kobayashi, R,A Normand, J,A Raghavachari, K,A Rendell, A. P,A Burant, J. C.A Iyengar, S. S.A Tomasi, J. A Cossi, M.A Millam, J. M.A Klene, M.A Adamo, C.A ammi, R.A Ochterski, J. W.A Martin, R. L.A Morokuma, K.A Farkas, O.A Foresman, J. B.A Fox, D. J.D 2016T Gaussian 16 Rev. C.01C Wallingford, CT Gaussian 16.

[23]   Kaya, R., & Kaya, C. (2018). "Theoretical study on the HOMO–LUMO gap and stability of enaminones using DFT." Journal of Molecular Structure, 1171, 290–297.

[24]   Guevara, P., et al. (2020). "DFT study on β-enaminones: solvent effects, electronic properties and potential bioactivity." Computational and Theoretical Chemistry, 1188, 112937.

[25]   Becke, Axel D. "Density-functional exchange-energy approximation with correct asymptotic behavior." Physical review A 38, no. 6 (1988): 3098.

[26] Lee, Chengteh, Weitao Yang, and Robert G. Parr. "Development of the Colle-Salvetti correlation-energy formula into a functional of the electron density." Physical review B 37, no. 2 (1988): 785.

[27] Saleem, H., S. Subashchandrabose, N. Ramesh Babu, and M. Syed Ali Padusha. "Vibrational spectroscopy investigation and density functional theory calculations on (E)-N′-(4-methoxybenzylidene) benzohydrazide." Spectrochimica Acta Part A: Molecular and Biomolecular Spectroscopy 143 (2015): 230-241.

[28] G.A. Zhurko and D.A. Zhurko, Chemcraft Program, Academic version1.5 (2004).

[29] Singh, Ranvijay Pratap, Kuldeep Singh, Sonia Sharma, and Arun Sethi. "Synthesis, crystal structure, conformational analysis, nonlinear optical property and computational study of novel pregnane derivatives." Journal of Molecular Structure 1095 (2015): 125-134.

[30] Rajkumar, M., P. Muthuraja, M. Dhandapani, and A. Chandramohan. "Supramolecular network through NH center dot center dot center dot O, OH center dot center dot center dot O and CH center dot center dot center dot O hydrogen bonding interaction and density functional theory studies of 4-methylanilinium-3-carboxy-4-hydroxybenzenesulphonate crystal." Journal of Molecular Structure 1153 (2018): 192-201.